NANO LETTERS

Letter

pubs.acs.org/NanoLett

Liposome-Based Engineering of Cells To Package Hydrophobic Compounds in Membrane Vesicles for Tumor Penetration

Junsung Lee,[†,∥] Jiyoung Kim,[‡,∥] Moonkyoung Jeong,[‡,∥] Hyoungjin Lee,[‡,∥] Unbyeol Goh,[‡,∥] Hyaeyeong Kim,[§,∥] Byungji Kim,[‡,∥] and Ji-Ho Park*[,†,‡,∥,⊥]

[†]Graduate School of Medical Science and Engineering, [‡]Department of Bio and Brain Engineering, [§]Department of Chemistry, [∥]Institute for Optical Science and Technology, and [⊥]Institute for the Nanocentury, Korea Advanced Institute of Science and Technology (KAIST), Daejeon 305-338, Republic of Korea

Supporting Information

ABSTRACT: Natural membrane vesicles (MVs) derived from various types of cells play an essential role in transporting biological materials between cells. Here, we show that exogenous compounds are packaged in the MVs by engineering the parental cells via liposomes, and the MVs mediate autonomous intercellular migration of the compounds through multiple cancer cell layers. Hydrophobic compounds delivered selectively to the plasma membrane of cancer cells using synthetic membrane fusogenic liposomes were efficiently incorporated into the membrane of MVs secreted from the cells and then transferred to neighboring cells via the MVs. This liposome-mediated MV engineering strategy allowed hydrophobic photosensitizers to significantly penetrate both spheroids and in vivo tumors, thereby enhancing the therapeutic efficacy. These results suggest that innate biological transport systems can be in situ engineered via synthetic liposomes to guide the penetration of chemotherapeutics across challenging tissue barriers in solid tumors.

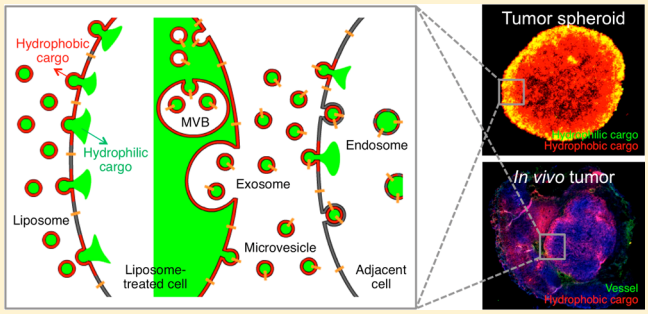

KEYWORDS: *Liposome, membrane vesicle, nanomedicine, photosensitizer, spheroid*

The major obstacle in increasing the efficacy of anticancer treatments lies in poor tumor penetration of therapeutic agents.[1,2] In solid tumors, high interstitial fluid pressure and dysfunctional lymphatic system impede delivery of therapeutic molecules into the deep parenchyma.[3] Nanoparticle formulations, including clinically approved PEGylated liposomal doxorubicin (Doxil) and albumin-bound paclitaxel (Abraxane), can alter the pharmacokinetics of drugs and take advantage of the enhanced permeability of tumor vessels, thereby improving tumor accumulation.[4,5] Physiochemical properties, including size,[6,7] surface charge,[8] and attachment of targeting ligands[9,10] have been optimized for enhanced tumor penetration efficiency. However, a substantial quantity of therapeutic compounds delivered systemically through the currently available nanocarriers remains predominantly in the perivascular region, reducing the overall therapeutic effect.

Membrane vesicles (MVs, 50−1000 nm in diameter), including exosomes and microvesicles, are endogenous particles secreted from many different cell types.[11,12] MVs participate in intercellular communications by delivering biological cargo to target cells.[13−15] They also play a crucial role in the development of cancer in that tumor-derived MVs mediate cancer progression and metastasis by transferring biological materials to local tumor-associated cells and remote tissues vulnerable to metastasis.[16−19] Recently, researchers prompted to isolate MVs from parental cells and further engineer them for therapeutic applications to leverage their endogenous origin and ability to package biological cargo.[20−22] However, the isolation and engineering procedures could be laborious and lead to damage of MVs. In contrary to such previous works wherein the isolated MVs were used as drug carriers, the MVs produced in the tumor microenvironment may be harnessed and reconfigured in situ to our own design to carry exogenous therapeutic compounds through multiple cell layers by taking advantage of innate intercellular migration mechanisms. Herein, we report that exogenous compounds can be efficiently packaged into MVs by engineering the parental cells using synthetic membrane fusogenic liposomes (MFLs) loaded with the compounds, and the MVs secreted from the engineered cells can autonomously migrate to surrounding cells, thereby enabling intercellular translocation of the compounds through multiple cell layers (Figure 1a). We also evaluated the therapeutic potential of MV-mediated tissue penetration of hydrophobic compounds in both spheroid and in vivo tumor models.

MVs include portions of the membrane and cytosol of parental cells. Thus, we first tested whether synthetic liposomes engineered to fuse with the plasma membrane could be used to

Received: December 10, 2014
Revised: March 23, 2015
Published: March 25, 2015

DOI: 10.1021/nl5047494
Nano Lett. 2015, 15, 2938−2944

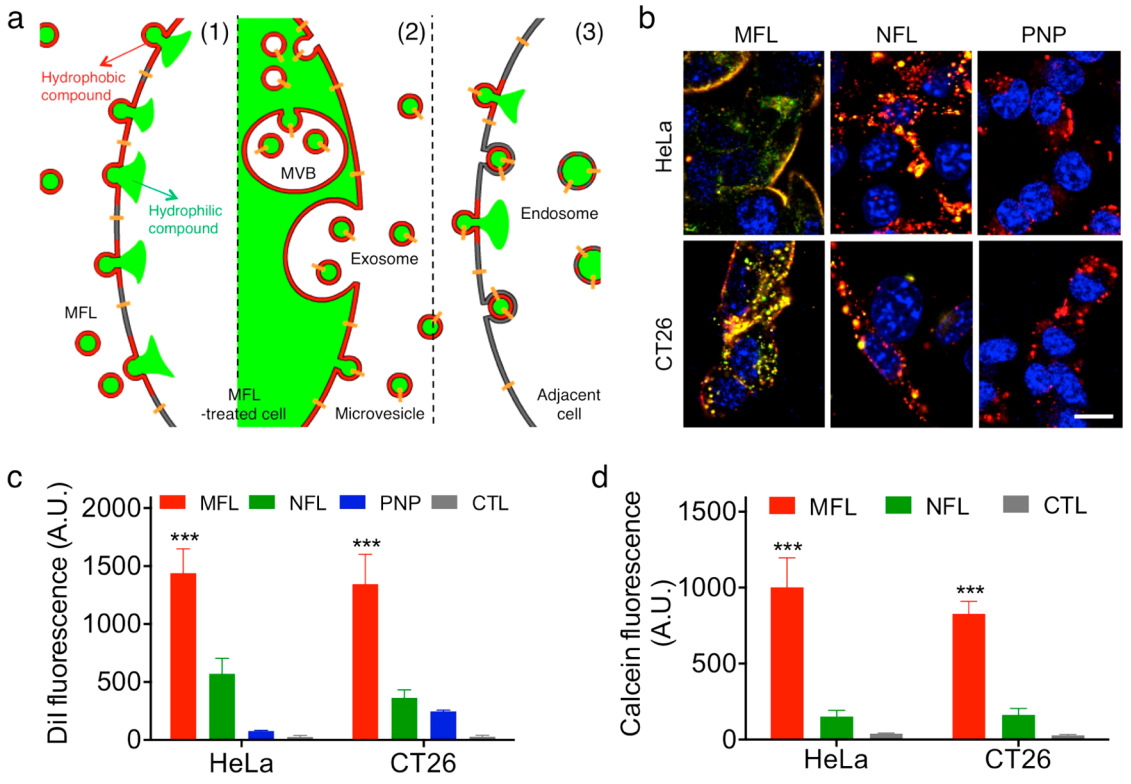

Figure 1. Incorporation of hydrophilic and hydrophobic compounds into membrane vesicles by engineering the parental cells via synthetic liposomes. (a) Schematic showing that membrane vesicles (MVs) including exosomes and microvesicles mediate delivery of hydrophilic and hydrophobic cargo to adjacent cells; (1) Membrane delivery of cargo by MFLs, (2) Secretion of cargo-loaded MVs from the cells and (3) MV-mediated delivery of cargo to adjacent cells. MVB denotes a multivesicular body. (b) Confocal microscopic images of HeLa and CT26 cancer cells treated with various synthetic nanoparticles coloaded with hydrophilic dye calcein (green) and hydrophobic dye DiI (red) for 30 min. Nuclei were stained with Hoechst (blue). (c and d) Fluorescence intensities of DiI (c) and calcein (d) in equal quantities of MVs secreted from cells treated with synthetic nanoparticles coloaded with DiI and calcein (MFL and NFL) or with DiI alone (PNP). MFL, NFL, and PNP denote membrane fusogenic liposomes, nonfusogenic liposomes, and poly(lactic-*co*-glycolic acid) nanoparticles, respectively. Scale bar indicates 5 μm. Data represent averages ± SD (n = 3–5, ***P < 0.001 by ANOVA).

package hydrophobic compounds into the membrane and hydrophilic compounds into the core of MVs (Figure 1a). Liposomal formulations with membrane fusogenic capabilities were prepared by varying lipid compositions and base lipids[23] (Supplementary Figures S1 and S2). Membrane fusogenicity was compared based on the degree to which the liposomal membrane merged with the plasma membrane. The L2 formulation was selected for all subsequent experiments, as they exhibited the highest membrane fusogenicity (Supplementary Figure S1b), and in turn, the most effective translocation of the hydrophobic/lipophilic dye 1,1′-dioctadecyl-3,3,3′,3′-tetramethylindocarbocyanine perchlorate (DiI) from the liposomal membrane to the plasma membrane (Supplementary Figures S1c and S2b).

Next, we examined intracellular delivery of cargo to cancer cells using synthetic nanoparticles. Conventional cationic liposomes (referred to here as nonfusogenic liposomes, NFLs) and poly(lactic-*co*-glycolic acid) nanoparticles (PNPs), which both carry payload into the cells via endocytosis, were prepared alongside MFLs for comparison (Table 1). As expected, NFLs fused less effectively with the plasma membrane of cancer cells than did MFLs (Supplementary Figure S3). Cancer cells were treated with synthetic nanoparticles coloaded with hydrophobic DiI and hydrophilic calcein (for MFLs and NFLs) or loaded with the DiI alone (for PNP) for 30 min. As a result, MFLs delivered the DiI to the plasma membrane and calcein into the cytoplasm. In contrast, NFLs and PNPs transferred both DiI and calcein into the endosome/lysosomes (Figure 1b and Supplementary Figures S3 and S4a). These results demonstrate that MFLs enable codelivery of hydrophobic and hydrophilic compounds into the cellular membrane and cytosol, respectively, largely bypassing the endosome/lysosome pathway.

We subsequently assessed whether cargo delivered into the subcellular regions of cancer cells via synthetic nanoparticles could be translocated into MVs. Two days after nanoparticle

Table 1. Lipid Compositions and Physical Properties of Synthetic Nanoparticles Used in This Study

	lipid composition (molar ratio)				
nanoparticle[a]	DMPC	PEG–PE	DOTAP	hydrodynamic size[b] (nm)	surface charge[c] (mV)
MFL	76.15	3.85	20	122.7	15.6
NFL	80	0	20	127.2	53.0
P-NFL	96.15	3.85	0	119.0	−5.4
PNP				99.5	−42.6

[a]MFL, NFL, P-NFL, and PNP denote membrane fusogenic liposomes, nonfusogenic liposomes, PEGylated nonfusogenic liposomes, and poly(lactic-*co*-glycolic acid) nanoparticles, respectively. [b]Mean hydrodynamic sizes of the nanoparticles based on dynamic light scattering measurements (n = 3). [c]Mean surface charges of the nanoparticles based on zeta-potential measurements (n = 3).

DOI: 10.1021/nl5047494
Nano Lett. 2015, 15, 2938–2944

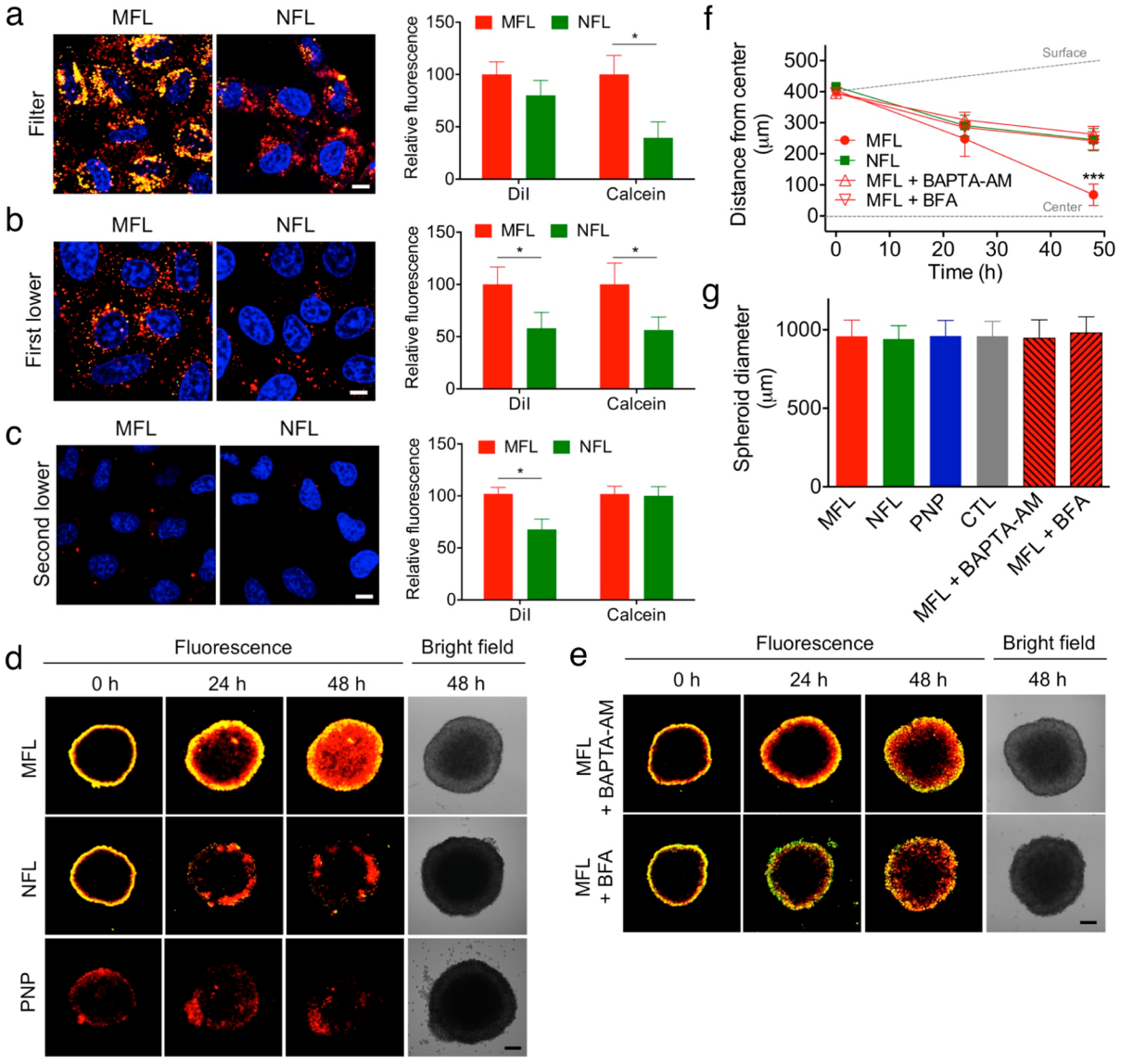

Figure 2. Intercellular migration of hydrophilic and hydrophobic compounds mediated by membrane vesicles. (a–c) Confocal microscopic images and fluorescence quantification of HeLa cells in the transwell filter (a), in the first lower chamber (b), and in the second lower chamber (c) after treatments with double cargo-loaded liposomes in the transwell filter. DiI (red) and calcein (green) fluorescence intensity in each chamber after NFL treatments were normalized to those in each chamber after MFL treatments. Nuclei were stained with Hoechst (blue). (d and e) Confocal and bright field microscopic images of HeLa spheroids treated with double cargo-loaded nanoparticles (d) or treated with double cargo-loaded nanoparticles followed by inhibitors (e). The spheroids were treated with MFLs or NFLs coloaded with DiI and calcein, or with PNPs loaded with DiI alone for 30 min and then washed (0 h). For (e), the nanoparticle-treated spheroids were further treated with agents to inhibit production of MVs (BAPTA-AM or BFA). (f) Quantification of DiI migration in (d) and (e) to assess spheroid penetration of DiI delivered to the spheroid periphery by synthetic nanoparticles. In each image, the mean distance that DiI migrated toward the center was measured based on DiI fluorescence. (g) Growth of spheroids treated with synthetic nanoparticles or with synthetic nanoparticles followed by inhibitors. Scale bars indicate 5 μm in (a–c) and 200 μm in (d–e). Data represent averages ± SD [$n = 4$ in (a–c) $^*P < 0.05$ using the nonparametric Mann–Whitney U test; $n = 5$ in (f), $n = 10$ in (g), $^{***}P < 0.001$ by ANOVA].

treatment, MVs secreted from the cells were purified from the culture supernatant using an established ultracentrifugation protocol for exosome isolation.[20] MFL treatment produced MVs loaded with higher quantities of both hydrophilic and hydrophobic agents, when compared with NFL and PNP treatments (Figure 1c and d). Other liposomal formulations, such as PEGylated nonfusogenic liposomes (P-NFLs, L4 formulation in Supplementary Figure S1) that are the most common liposomal formulation for tumor-specific drug delivery,[24] exhibited inefficient cargo incorporation into the MVs due to their poor membrane fusion (Supplementary Figure S5). Notably, the hydrophobic compounds transferred to the plasma membrane via MFLs were minimally associated with the lysosomal pathway, incorporated into the Golgi membrane, which participates in exosome biogenesis,[25] and finally packaged into the membrane of MVs (Supplementary Figure S4). Interestingly, endothelial cells and macrophages showed inefficient packaging of the hydrophobic compounds into their MVs due to poor cellular uptake (endothelial cells) and membrane fusion (macrophages) of MFLs (Supplementary Figure S6), suggesting that the MFL-based intracellular packaging favor the cancer cells. Nanoparticle treatment did

DOI: 10.1021/nl5047494
Nano Lett. 2015, 15, 2938–2944

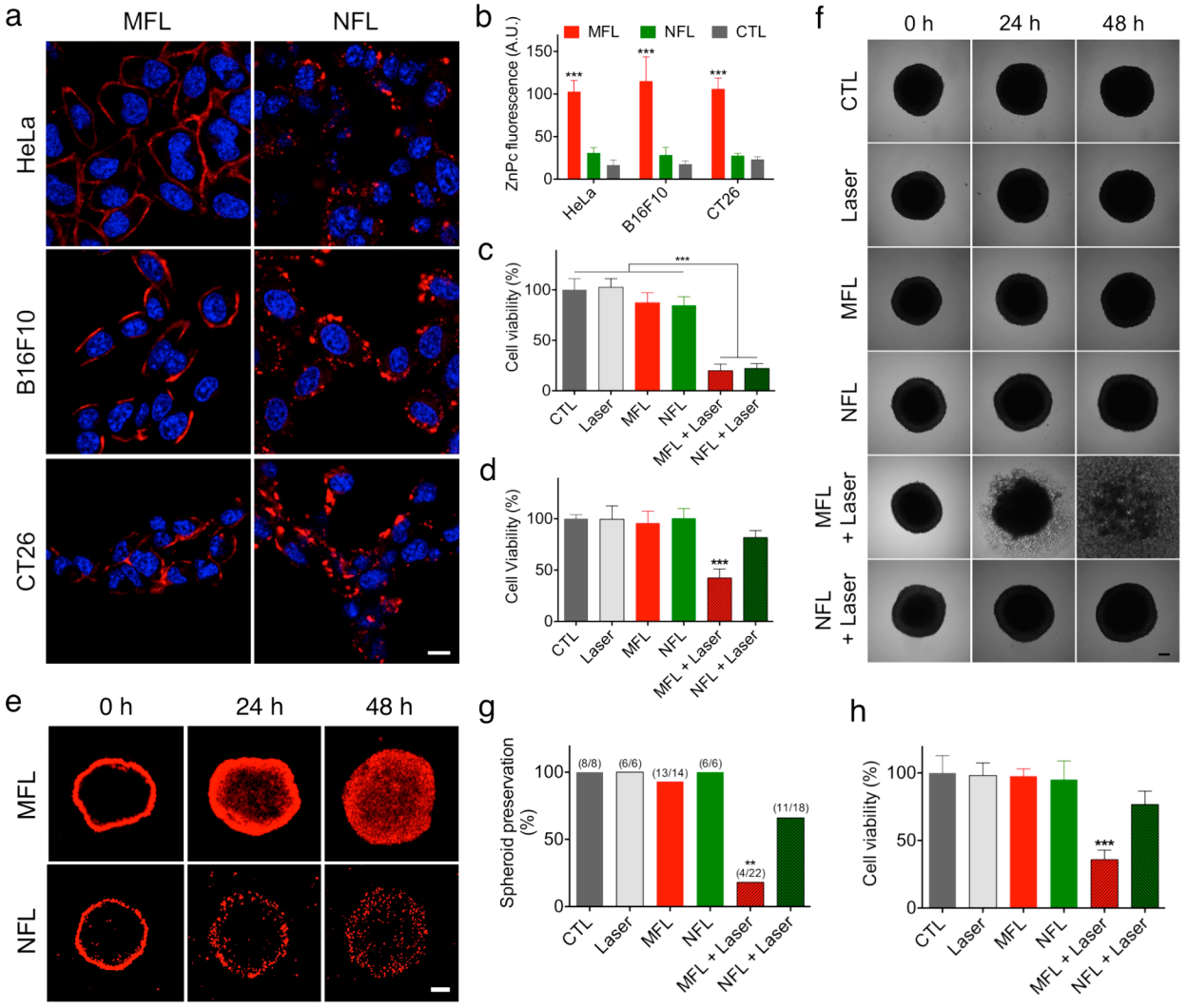

Figure 3. Membrane vesicle-mediated delivery of hydrophobic photosensitizers for in vitro photodynamic therapy. (a) Confocal microscopic images of cancer cells treated with liposomes loaded with the hydrophobic photosensitizer ZnPc (red). Nuclei were stained with Hoechst (blue). The scale bar indicates 5 μm. (b) ZnPc fluorescence intensity from equal amounts of MVs produced from cells over a 48-h period after 30 min treatments with ZnPc-loaded liposomes. (c and d) Photodynamic therapy of HeLa cells in the transwell filter (c) and the lower chamber (d) of a transwell after treatment with ZnPc-loaded liposomes. Cell viability was analyzed by MTT assay. (e) Confocal microscopic images of HeLa tumor spheroids treated with ZnPc-loaded liposomes. The spheroids were treated with ZnPc-loaded liposomes for 30 min, washed (0 h), and further incubated for 48 h. (f–h) Photodynamic therapy of HeLa spheroids treated with ZnPc-loaded liposomes. Bright field microscopic images (f), preservation (g), and cell viability (h) of the ZnPc-treated spheroids over a 48 h period of time after laser irradiations. Scale bars in (e) and (f) indicate 200 μm. Data represent averages ± SD [n = 3–5 in (b), n = 6–12 in (c and d), n = 6–9 in (h), ***P < 0.001 by ANOVA; n = 6–22 in (g) **P < 0.01 by chi-square test].

not influence amount and physiochemical properties of MVs secreted (Supplementary Figure S7), indicating no cytotoxicity induced by the nanoparticles.

After establishing intracellular loading of exogenous compounds in the MVs, we examined MV-mediated intercellular migration of compounds in both HeLa and CT26 cancer cells using transwell systems (Figure 2a–c and Supplementary Figure S8a–c). Cancer cells in the first transwell filter, treated with synthetic liposomes coloaded with calcein and DiI for 30 min, were coincubated with fresh cells in the first lower chamber for 48 h in order to observe cargo translocation. Cells in the first lower chamber were then replated onto another transwell filter without additional treatment and coincubated with fresh cells in the lower chamber of the second transwell system for 48 h. At 48 h post-treatment, the amount of calcein remaining in the cells in the transwell filter was significantly higher with the MFL treatment than with the NFL treatment, while that of DiI was similar to both treatments. In both lower chambers, significantly higher quantities of DiI were translocated from the MFL-treated cells of the filter compared with the NFL-treated cells. Higher quantities of calcein were also observed in the first lower chamber cells of the MFL-treated transwell. To further confirm that MVs mediated intercellular migration of compounds, MVs were removed from the supernatant collected from liposome-treated cells, and fresh cells were treated with the MV-depleted supernatant. Neither DiI nor calcein was observed in the treated cells (Supplementary Figure S9), indicating that the intercellular translocation of compounds was mediated by cell-derived MVs. These results indicate that hydrophobic compounds delivered to the plasma membrane can be secreted from the cells by effective incorporation into MV membranes and subsequently transferred to adjacent cells. In contrast, the quantity of hydrophilic compounds being transferred to neighboring cells

DOI: 10.1021/nl5047494
Nano Lett. 2015, 15, 2938–2944

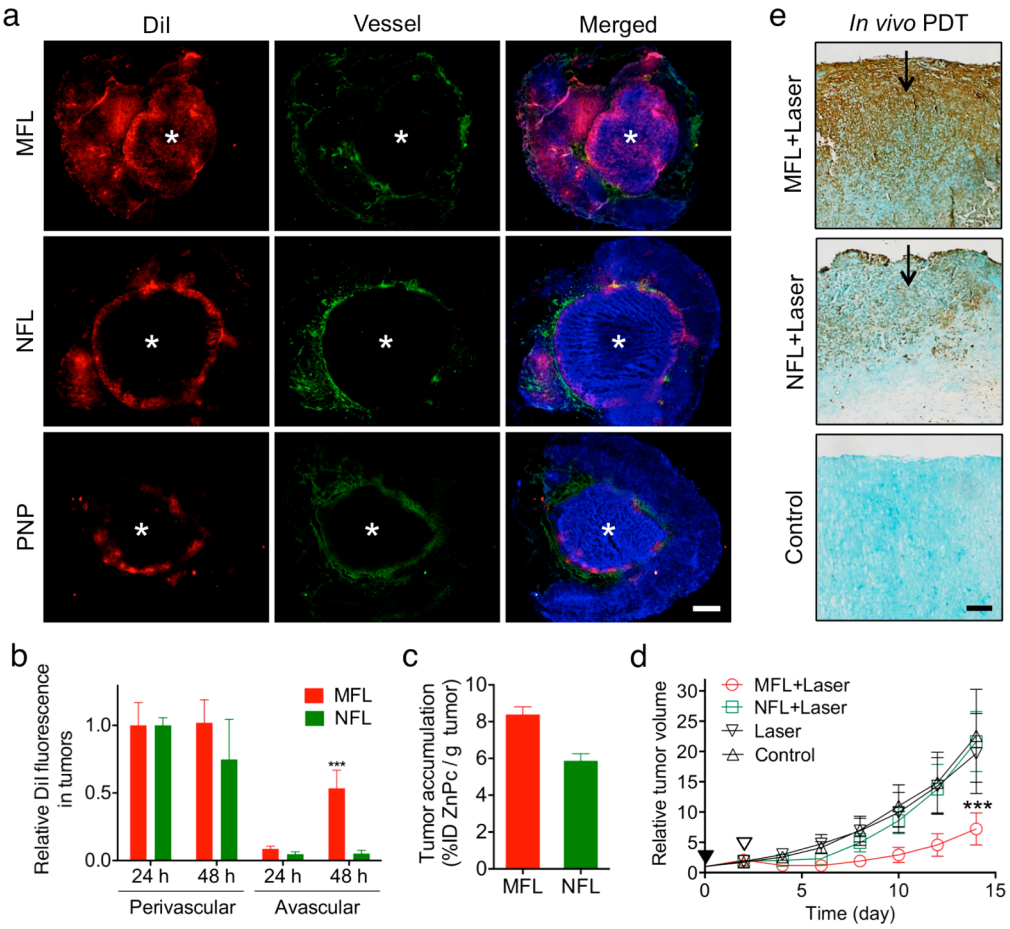

Figure 4. Liposome-mediated engineering of MVs in the tumor microenvironment for tumor penetration of hydrophobic compounds and its application for in vivo photodynamic therapy. (a) Fluorescence images of CT26 tumor sections 48 h after intravenous injection of DiI(red)-loaded nanoparticles. Nuclei were stained with Hoechst (blue) and vessels with CD31 (green). Scale bar indicates 500 μm. * indicates an avascular region. (b) Quantitative analysis of time-dependent migration of DiI in the tumor tissues after intravenous injection of DiI-loaded liposomes. (c) Quantification of the ZnPc amount accumulated in the tumor 48 h after intravenous injection of ZnPc-loaded liposomes. (d) Tumor growth inhibition by photodynamic therapy with MV-mediated penetration of ZnPc in CT26 tumors. No significant difference was observed in the starting tumor volumes among groups (average volume of starting tumors: ~45 mm^3). Solid and hollow arrowheads indicate liposome injection and laser irradiation, respectively. (e) Histological observation of apoptotic cells in the tumors using TUNEL staining. Arrows indicate the direction of laser irradiation used for photodynamic therapy. Scale bar indicates 200 μm. Data represent averages ± SD [n = 3–5 in (b), n = 6–10 in (d), ***P < 0.001 by ANOVA].

diminished with each transfer, possibly due to degradation via the endosome/lysosome pathway.

Next, we chose a multicellular tumor spheroid model to study MV-mediated penetration of compounds through multiple cell layers, because this model mimics the three-dimensional cell masses populated amid blood vessels in vivo.[26] HeLa or CT26 tumor spheroids were treated with liposomes coloaded with DiI and calcein or with PNP loaded with DiI alone for 30 min, and further incubated for 48 h. Substantial migration of DiI from the periphery into the center was observed in the MFL-treated spheroids when compared with the NFL- and PNP-treated spheroids (Figure 2d–f and Supplementary Figure S8d–f). In contrast, calcein was primarily immobilized in the outer cell layers of both MFL- and NFL-treated spheroids, although it was retained longer in the cells of MFL-treated spheroids. If the MFLs themselves or MVs secreted from the peripheral cells had penetrated to the core of the spheroid, the calcein should also have been observed in the center. However, only the DiI could be observed, leading us to believe that the hydrophobic compounds delivered by MFLs penetrate the spheroid by successive rounds of cellular uptake and subsequent MV production, rather than spheroid penetration of MFLs or a single round of MV production and their subsequent diffusion. The intercellular migration of DiI in the MFL-treated spheroids was significantly reduced either in the presence of inhibitors of MV secretion (BAPTA-AM[27] or brefeldin A[28]) or by blocking the expression of Rab GTPases that regulate exosome secretion[29] or ADP-ribosylation factor 6 (ARF6) that regulates microvesicle secretion[30] (Figure 2e–f, Supplementary Figure S8e–f and S10a–b). Furthermore, marked penetration of DiI was also observed in the spheroid treated with DiI-loaded MVs (produced from the cells treated with DiI-loaded MFLs) (Supplementary Figure S11). Collectively, the results from the spheroid experiments in conjunction with the transwell studies support the notion that MVs play a key role in intercellular migration of exogenous hydrophobic compounds through multiple cell layers. None of the treatments significantly influenced the spheroid growth (Figure 2g, Supplementary Figure S8g and S10c).

Since substantial intercellular migration of hydrophobic compounds delivered to the plasma membrane was observed

DOI: 10.1021/nl5047494
Nano Lett. 2015, 15, 2938–2944

in both cells and spheroids, we next assessed the therapeutic potential of MV-mediated delivery of a hydrophobic photosensitizer for photodynamic therapy (PDT). Cancer cells were treated with liposomes loaded with the hydrophobic photosensitizer zinc phthalocyanine (ZnPc) for 30 min, and MVs were isolated from the treated cells over a 48 h period. Intrinsic fluorescence of ZnPc delivered via MFLs was localized primarily in the plasma membrane, while that delivered via NFLs was localized presumably in endosomes (Figure 3a). As expected, MFL treatment produced MVs loaded with significantly higher quantities of ZnPc molecules compared with the NFL treatment (Figure 3b). In the transwell experiments, cells in the transwell filter treated with ZnPc-loaded liposomes for 30 min were coincubated with fresh cells plated on the lower chamber for 48 h. The cells in the filter and lower chamber were then irradiated separately using a 660 nm laser, and the cell viability was examined using MTT assay. Cells in the filter exhibited similar phototoxicity regardless of the liposome types treated, while cells in the lower chamber displayed significantly higher phototoxicity with the MFL +Laser treatment (Figure 3c–d and Supplementary Figure S12a–b). Thus, we can deduce that MVs produced from MFL-treated cells delivered higher quantities of ZnPc molecules to adjacent cells than did those from NFL-treated cells. Subsequently, tumor spheroids were treated with ZnPc-loaded liposomes for 30 min and incubated for 48 h. Substantial penetration of ZnPc was observed in the MFL-treated spheroids compared with the NFL-treated spheroids (Figure 3e). For PDT, liposome-treated spheroids were irradiated using a 660 nm laser, and examined for phototoxicity. In HeLa spheroids, the MFL+Laser treatment caused significant disintegration of the spheroids compared with the NFL +Laser treatment (Figure 3f–g). In CT26 spheroids, the spheroid size was significantly reduced by the MFL+Laser treatment, but remained unchanged by the NFL+Laser treatment (Supplementary Figure S12c–d). At 48 h (HeLa) or 72 h (CT26) postirradiation, spheroids were trypsinized to dissociate into individual cells, and the cell viability was examined. In both spheroids, the MFL+Laser treatment induced significantly higher phototoxicity compared with the NFL+Laser treatment (Figure 3h and Supplementary Figure S12e). Moreover, cell death was observed throughout the entire spheroid after MFL+Laser treatment, but not after NFL+Laser treatment (Supplementary Figure S13). Collectively, these observations suggest that hydrophobic photosensitizers delivered to the plasma membrane of the outermost cell layer spread throughout the entire spheroid over a 48-h period via intercellular migration of MVs, resulting in significant therapeutic effects under irradiation.

Having verified the MV-mediated intercellular migration of hydrophobic compounds in transwell and spheroid systems, we last examined its feasibility in tumors in vivo. To examine tumor-penetrating delivery of hydrophobic compounds, DiI-loaded nanoparticles were intravenously injected into mice bearing CT26 tumors. At 24 or 48 h postinjection, the tumor sections were imaged to observe time-dependent tumor distribution of DiI. Histological analysis revealed that the DiI delivered to the perivascular regions via MFLs migrated dramatically toward the avascular region over time (Figure 4a and b). Importantly, DiI fluorescence was detected throughout the entire tumor at 48 h postinjection. In contrast, DiI delivered via NFLs and PNPs accumulated predominantly near the blood vessels where they remained throughout a 48 h period. No significant difference was observed among the vessel densities in the tumors treated with various nanoparticles (Supporting Information, Figure S14). A similar pattern of tumor distribution of DiI was seen in MDA-MB-231 human breast tumors 48 h postinjection. (Supplementary Figure S15). When MFLs coloaded with calcein and DiI were intravenously injected, the distribution of calcein and DiI in the tumor tissue at 48 h after injection differed. Hydrophilic calcein remained at the focal region, considered as the vessel area, but DiI diffused through the broad tumor tissue as they did in the spheroid model, implying that tumor-penetrating delivery of hydrophobic compounds is not mediated by the liposome itself, but presumably mediated by MVs (Supporting Information, Figure S16). The MFLs retained their size in the physiological condition over an incubation period of 48 h without significant leakage of the loaded DiI, deducing its solid stability during circulation (Supplementary Figure S17).

For evaluation of PDT in vivo, CT26 tumors with an average volume of about 45 mm^3 were irradiated with a single dose of a 660 nm laser 2 days after intravenous injection of ZnPc-loaded liposomes, and their volumes were measured over 2 weeks. The amount of ZnPc delivered to the tumor via MFLs was slightly higher than that via NFLs (Figure 4c). The MFL treatment induced a significant reduction in tumor growth after irradiation compared with untreated, irradiated, and NFL-treated tumors (Figure 4d). The NFL-treated tumors displayed a slight delay of tumor growth the first few days postirradiation, but they subsequently began growing at a rate similar to the untreated tumors. TUNEL analysis using histological samples revealed that MFL+Laser treatment induced significant apoptosis in the irradiated region of tumor tissues compared with NFL+Laser treatment (Figure 4e). The MFL treatment also exhibited superior phototherapeutic effects compared with the P-NFL treatment, although the P-NFLs were likely to deliver ~2-fold greater quantity of photosensitizers to the tumor region (Supplementary Figure S18). For all of the treatments evaluated in this work, no significant loss in body mass was observed.

This work demonstrated that MVs, a natural transport system, can be in situ engineered via synthetic liposomes to mediate intercellular migration of exogenous hydrophobic compounds through multiple cell layers both in vitro and in vivo. This MV-mediated delivery approach would significantly improve the therapeutic efficacy of hydrophobic compounds in poorly vascularized tumors.[31,32] This work provides new insights to overcome the challenges associated with the delivery and penetration of chemotherapeutics across cell and tissue barriers.

■ ASSOCIATED CONTENT

Supporting Information

Methods and figures. This material is available free of charge via the Internet at http://pubs.acs.org.

■ AUTHOR INFORMATION

Corresponding Author

*E-mail: jihopark@kaist.ac.kr.

Present Address

J.L.: Department of Ophthalmology, Chonnam National University Medical School and Hospital, Gwangju 501-757, Republic of Korea.

DOI: 10.1021/nl5047494
Nano Lett. 2015, 15, 2938–2944

Author Contributions

J.L. and J.K. contributed equally. J.L., J.K., and J.-H.P. conceived and designed the research. J.L., J.K., M.J., H.L., U.G., H.K., and J.-H.P. carried out the experiments. J.L., J.K., M.J., B.K., and J.-H.P. analyzed the data. J.L. and J.-H.P. wrote the manuscript.

Notes

The authors declare no competing financial interest.

■ ACKNOWLEDGMENTS

This work was supported by the Basic Science Research Program (Grant No. NRF-2012R1A1A1011058), the Global Frontier Project (Grant No. NRF-2013M3A6A4072541), and the Pioneer Research Center Program (Grant No. NRF-2014M3C1A3051460) through the National Research Foundation funded by the Ministry of Science, ICT & Future Planning, Republic of Korea. The authors thank Y. Jeong for assistance with confocal fluorescence microscopy.

■ ABBREVIATIONS

MV, membrane vesicles; MFL, membrane fusogenic liposomes; NFL, nonfusogenic liposomes; PNP, poly(lactic-*co*-glycolic acid) nanoparticles; PEG, polyethylene glycol; DiI, 1,1′-dioctadecyl-3,3,3′,3′-tetramethylindocarbocyanine perchlorate; BAPTA-AM, 1,2-Bis(2-aminophenoxy)ethane-N,N,N′,N′-tetra-acetic acid tetrakis(acetoxymethyl ester); ARF6, ADP-ribosylation factor 6; PDT, photodynamic therapy; ZnPc, zinc phthalocyanine

■ REFERENCES

(1) Jain, R. K.; Stylianopoulos, T. *Nat. Rev. Clin. Oncol.* **2010**, *7*, 653−664.
(2) Ruoslahti, E.; Bhatia, S. N.; Sailor, M. J. *J. Cell Biol.* **2010**, *188*, 759−768.
(3) Minchinton, A. I.; Tannock, I. F. *Nat. Rev. Cancer* **2006**, *6*, 583−592.
(4) Northfelt, D. W.; Dezube, B. J.; Thommes, J. A.; Miller, B. J.; Fischl, M. A.; Friedman-Kien, A.; Kaplan, L. D.; Du Mond, C.; Mamelok, R. D.; Henry, D. H. *J. Clin. Oncol.* **1998**, *16*, 2445−51.
(5) Gradishar, W. J.; Tjulandin, S.; Davidson, N.; Shaw, H.; Desai, N.; Bhar, P.; Hawkins, M.; O'Shaughnessy, J. *J. Clin. Oncol.* **2005**, *23*, 7794−7803.
(6) Perrault, S. D.; Walkey, C.; Jennings, T.; Fischer, H. C.; Chan, W. C. W. *Nano Lett.* **2009**, *9*, 1909−1915.
(7) Cabral, H.; Matsumoto, Y.; Mizuno, K.; Chen, Q.; Murakami, M.; Kimura, M.; Terada, Y.; Kano, M. R.; Miyazono, K.; Uesaka, M.; Nishiyama, N.; Kataoka, K. *Nat. Nanotechnol.* **2011**, *6*, 815−823.
(8) Kim, B.; Han, G.; Toley, B. J.; Kim, C.-k.; Rotello, V. M.; Forbes, N. S. *Nat. Nanotechnol.* **2010**, *5*, 465−472.
(9) Sugahara, K. N.; Teesalu, T.; Karmali, P. P.; Kotamraju, V. R.; Agemy, L.; Greenwald, D. R.; Ruoslahti, E. *Science* **2010**, *328*, 1031−1035.
(10) Ren, Y.; Cheung, H. W.; von Maltzhan, G.; Agrawal, A.; Cowley, G. S.; Weir, B. A.; Boehm, J. S.; Tamayo, P.; Karst, A. M.; Liu, J. F.; Hirsch, M. S.; Mesirov, J. P.; Drapkin, R.; Root, D. E.; Lo, J.; Fogal, V.; Ruoslahti, E.; Hahn, W. C.; Bhatia, S. N. *Sci. Transl. Med.* **2012**, *4*, 147ra112.
(11) Thery, C.; Zitvogel, L.; Amigorena, S. *Nat. Rev. Immunol.* **2002**, *2*, 569−579.
(12) Thery, C.; Ostrowski, M.; Segura, E. *Nat. Rev. Immunol.* **2009**, *9*, 581−593.
(13) Valadi, H.; Ekstrom, K.; Bossios, A.; Sjostrand, M.; Lee, J. J.; Lotvall, J. O. *Nat. Cell Biol.* **2007**, *9*, 654−659.
(14) Gross, J. C.; Chaudhary, V.; Bartscherer, K.; Boutros, M. *Nat. Cell Biol.* **2012**, *14*, 1036−1045.
(15) Mittelbrunn, M.; Sánchez-Madrid, F. *Nat. Rev. Mol. Cell Biol.* **2012**, *13*, 328−335.
(16) Skog, J.; Wurdinger, T.; van Rijn, S.; Meijer, D. H.; Gainche, L.; Curry, W. T.; Carter, B. S.; Krichevsky, A. M.; Breakefield, X. O. *Nat. Cell Biol.* **2008**, *10*, 1470−1476.
(17) Hood, J. L.; San, R. S.; Wickline, S. A. *Cancer Res.* **2011**, *71*, 3792−3801.
(18) Luga, V.; Zhang, L.; Viloria-Petit, A. M.; Ogunjimi, A. A.; Inanlou, M. R.; Chiu, E.; Buchanan, M.; Hosein, A. N.; Basik, M.; Wrana, J. L. *Cell* **2012**, *151*, 1542−1556.
(19) Peinado, H.; Aleckovic, M.; Lavotshkin, S.; Matei, I.; Costa-Silva, B.; Moreno-Bueno, G.; Hergueta-Redondo, M.; Williams, C.; Garcia-Santos, G.; Ghajar, C. M.; Nitadori-Hoshino, A.; Hoffman, C.; Badal, K.; Garcia, B. A.; Callahan, M. K.; Yuan, J.; Martins, V. R.; Skog, J.; Kaplan, R. N.; Brady, M. S.; Wolchok, J. D.; Chapman, P. B.; Kang, Y.; Bromberg, J.; Lyden, D. *Nat. Med.* **2012**, *18*, 883−891.
(20) Alvarez-Erviti, L.; Seow, Y.; Yin, H.; Betts, C.; Lakhal, S.; Wood, M. J. A. *Nat. Biotechnol.* **2011**, *29*, 341−345.
(21) Ohno, S.; Takanashi, M.; Sudo, K.; Ueda, S.; Ishikawa, A.; Matsuyama, N.; Fujita, K.; Mizutani, T.; Ohgi, T.; Ochiya, T.; Gotoh, N.; Kuroda, M. *Mol. Ther.* **2013**, *21*, 185−91.
(22) El Andaloussi, S.; Mager, I.; Breakefield, X. O.; Wood, M. J. A. *Nat. Rev. Drug Discov.* **2013**, *12*, 347−357.
(23) Gopalakrishnan, G.; Danelon, C.; Izewska, P.; Prummer, M.; Bolinger, P.-Y.; Geissbühler, I.; Demurtas, D.; Dubochet, J.; Vogel, H. *Angew. Chem., Int. Ed.* **2006**, *45*, 5478−5483.
(24) Woodle, M. C. *Adv. Drug Delivery Rev.* **1995**, *16*, 249−265.
(25) Laulagnier, K.; Vincent-Schneider, H.; Hamdi, S.; Subra, C.; Lankar, D.; Record, M. *Blood Cell. Mol. Dis.* **2005**, *35*, 116−121.
(26) Friedrich, J.; Seidel, C.; Ebner, R.; Kunz-Schughart, L. *Nat. Protocols* **2009**, *4*, 309−324.
(27) Savina, A.; Furlán, M.; Vidal, M.; Colombo, M. I. *J. Biol. Chem.* **2003**, *278*, 20083−20090.
(28) Mittelbrunn, M.; Gutierrez-Vazquez, C.; Villarroya-Beltri, C.; Gonzalez, S.; Sanchez-Cabo, F.; Gonzalez, M. A.; Bernad, A.; Sanchez-Madrid, F. *Nat. Commun.* **2011**, *2*, 282.
(29) Ostrowski, M.; Carmo, N. B.; Krumeich, S.; Fanget, I.; Raposo, G.; Savina, A.; Moita, C. F.; Schauer, K.; Hume, A. N.; Freitas, R. P.; Goud, B.; Benaroch, P.; Hacohen, N.; Fukuda, M.; Desnos, C.; Seabra, M. C.; Darchen, F.; Amigorena, S.; Moita, L. F.; Thery, C. *Nat. Cell Biol.* **2010**, *12*, 19−30.
(30) Muralidharan-Chari, V.; Clancy, J.; Plou, C.; Romao, M.; Chavrier, P.; Raposo, G.; D'Souza-Schorey, C. *Curr. Biol.* **2009**, *19*, 1875−1885.
(31) Olive, K. P.; Jacobetz, M. A.; Davidson, C. J.; Gopinathan, A.; McIntyre, D.; Honess, D.; Madhu, B.; Goldgraben, M. A.; Caldwell, M. E.; Allard, D.; Frese, K. K.; DeNicola, G.; Feig, C.; Combs, C.; Winter, S. P.; Ireland-Zecchini, H.; Reichelt, S.; Howat, W. J.; Chang, A.; Dhara, M.; Wang, L.; Rückert, F.; Grützmann, R.; Pilarsky, C.; Izeradjene, K.; Hingorani, S. R.; Huang, P.; Davies, S. E.; Plunkett, W.; Egorin, M.; Hruban, R. H.; Whitebread, N.; McGovern, K.; Adams, J.; Iacobuzio-Donahue, C.; Griffiths, J.; Tuveson, D. A. *Science* **2009**, *324*, 1457−1461.
(32) Provenzano, P. P.; Cuevas, C.; Chang, A. E.; Goel, V. K.; Von Hoff, D. D.; Hingorani, S. R. *Cancer Cell* **2012**, *21*, 418−429.

DOI: 10.1021/nl5047494
Nano Lett. 2015, 15, 2938−2944